Enzymatic hydrolysis of amylopectins from lotus rhizome and kudzu starches

LI GUO – HUI LI – BO CUI

Summary
To elucidate the influence of chain distributions on enzymatic digestibility of lotus rhizome and kudzu amylopectins, the correlation between the chain length distribution and enzymatic hydrolysis of amylopectins was studied. The results indicated that lotus rhizome amylopectin was more susceptible to amylase hydrolysis than kudzu amylopectin since lotus rhizome amylopectin contained a higher proportion of short chains. Using α-amylase and glucoamylase, individually or in combination, the values of digestion rate constant *k* of kudzu amylopectin were lower than that of lotus rhizome amylopectin. A small amount of glucose was released from kudzu and lotus rhizome amylopectins with α-amylase alone, whereas the release of glucose remarkably increased with α-amylase and glucoamylase. It confirmed that the synergism existed between α-amylase and glucoamylase in glucose released from kudzu and lotus rhizome amylopectins. The chain length distribution of amylopectins significantly affected the hydrolysis of amylases and they were highly correlated with the digestibility properties of lotus rhizome and kudzu starches.

Keywords
chain length distribution; kudzu amylopectin; lotus rhizome amylopectin; amylase hydrolysis

Kudzu (*Pueraria lobata*) and lotus (*Nelumbo Nucifera*) are two well-known medicinal starch sources. The plants are widely cultivated in East Asian countries, such as China, Korea or Japan. For many years, both kudzu and lotus have been considered the root plants of high nutritional value used for health care including diuretic, antiemetic, antidote in the treatment of tissue inflammation and cancer, and treating fever, diarrhoea, dysentery, diabetes, dizziness or cerebrovascular diseases [1, 2]. Kudzu and lotus starches are isolated from the root and lotus rhizome, the yields of starches being approximately 15–35 g·kg^{-1} and 10–20 g·kg^{-1} for both fresh root and rhizome, respectively [3]. Kudzu and lotus rhizome starches have become a very popular functional food in China and have been widely used as a nutritive powder, breakfast, fast food, traditional confectionery and food additive. It is expected that the eating and nutritional quality of kudzu and lotus foods depend greatly on the starch quality, especially for the property of good digestibility [4, 5]. Starch consists of amylose containing a linear polymer of α-D-glucose units linked by α-1, 4 glycosidic linkages, and amylopectin possessing a branched polymer of α-D-glucose units linked by α-1, 4 and α-1, 6 glycosidic linkages [6]. Generally, normal starches contain 70–80 g·kg^{-1} amylopectin and 20–30 g·kg^{-1} amylose [7]. It was reported that kudzu and lotus rhizome starches contain 20–23 g·kg^{-1} and 19–25 g·kg^{-1} amylose, respectively [8, 9]. Currently, most studies focus on the effects of starch granular size and shape, amylose content, the ratio of amylose to amylopectin, type and degree of crystallinity on the enzymatic hydrolysis of kudzu and lotus rhizome starches [5, 10, 11]. It was been reported that the chain length distribution of amylopectins are closely relevant to physico-chemical properties and digestibility of starch [12–16]. Amylopectin chains are classified as external and internal [12]. External chains interact with each other to form crystalline lamellae consisting of double helices. Internal chains exist in the amorphous lamellae composed of clusters

Li Guo, Hui Li, Bo Cui, State Key Laboratory of Biobased Material and Green Papermaking, School of Food Sciences and Engineering, Qilu University of Technology (Shandong Academy of Sciences), No. 3501 Daxue Road, Changqing District, 250353 Jinan, China.

Correspondence author
Bo Cui, tel.: +86-186-60811718; fax: +86-531-89631195, e-mail: cuiborr@163.com

of branches [14, 15, 17]. It is noteworthy that the internal structure of amylopectin including cluster and ϕ,β-limit dextrin structures is closely related to the enzymatic hydrolysis of starch [12, 16]. However, the correlation between the chain length distribution and enzymatic hydrolysis of amylopectins has not been widely reported. α-Amylase and glucoamylase, as endo-acting and exo-acting enzymes, respectively, are extensively utilized to investigate starch hydrolysis [18]. In this context, it is important to elucidate the effects of the internal molecular structure of kudzu and lotus rhizome starches on their digestibility in order to explore a nutritional ingredient in functional foods. In this study, the chain length distribution of kudzu and lotus rhizome amylopectins was comparatively analysed using high-performance anion-exchange chromatography with pulsed amperometric detection (HPAEC-PAD). Then, based on the chain length distribution of amylopectin, the susceptibility of kudzu and lotus rhizome amylopectins to α-amylase from *Bacillus amyloliquefaciens*, or in combination with glucoamylase from *Aspergillus niger*, was studied using logarithm of slope analysis, ultraviolet spectrophotometry and high-performance liquid chromatography (HPLC) to describe the relationship between the chain length distribution and enzymatic hydrolysis of amylopectins.

MATERIALS AND METHODS

Kudzu and lotus rhizome starches were obtained from Geye Starch (Anhui, China) and Zhoushi Food (Guangxi, China), respectively. The starches were defatted with methanol (85 %, v/v) and then were deproteinized with chloroform/*n*-butanol (4 : 1, v/v). Barley β-amylase (EC 3.2.1.2, 460 U·ml^{-1}), α-amylase from *Bacillus amyloliquefaciens* (EC 3.2.1.1, 420 U·ml^{-1}), glucoamylase from *Aspergillus niger* (EC 3.2.1.3, 340 U·ml^{-1}), rabbit muscle phosphorylase α (EC 2.4.1.1, 110 U·ml^{-1}) and isoamylase (EC 3.2.1.68, 160 000 U·ml^{-1}) from *Pseudomonas amyloderamosa* were obtained from Sigma-Aldrich (St. Louis, Missouri, USA). Promozyme D2 (EC 3.2.1.41, 1 350 U·ml^{-1}) was kindly donated by Novozymes (Copenhagen, Denmark). D-(+)-Maltose monohydrate standard and the reagents used in the colorimetric determination of reducing sugars (3,5-dinitrosalicylic acid, DNS) were from Sigma-Aldrich. Glucose, maltose, maltotriose, maltotetraose, maltopentaose, maltohexaose and maltoheptaose were obtained from Sigma-Aldrich.

Amylase activity assay

Amylase activity was analysed by quantifying reducing sugars on the basis of the Somogyi-Nelson method [19]. Soluble starch (1.0 mg·ml^{-1}) was as substrate in 100 mmol·l^{-1} sodium maleate buffer (pH 6.0) containing 5.0 mmol·l^{-1} calcium chloride at 35 °C [20]. Maltose (0–0.001 mol·l^{-1}) was used as a standard. The results were represented as micromoles of maltose equivalents released per minute and per millilitre at 35 °C. One unit (U) means the amount of enzyme releasing 1.0 μmol maltose per millilitre from soluble starch per minute at 35 °C and pH 6.0.

Extraction and purification of amylopectins

Amylopectins were extracted and purified by previously published methods with minor modifications [2]. Kudzu or lotus rhizome starch was added to 50 ml of 90% (v/v) dimethyl sulfoxide and then stirred uniformly and heated at 100 °C for 60 min. The gelatinized solution was cooled to room temperature and then 300 ml of absolute ethanol was added with continuous stirring for 20 min and centrifuged at 100 Hz for 5 min. The sediment was washed with 150 ml absolute ethanol and then centrifuged at 6 000 ×*g* for 5 min. The precipitate was dispersed in 100 ml of 90% dimethyl sulfoxide, heated at 100 °C with constant stirring for 30 min and then cooled to room temperature. A volume of 400 ml distilled water containing 6% (v/v) 1-butanol and 6% (v/v) isoamylalcohol was added to the mixed solution and stirred at 100 °C for 60 min, and then the mixture was cooled to room temperature. The mixed solution was centrifuged at 10 000 ×*g* for 15 min. The supernatant was concentrated to 60 ml at 40 °C under vacuum using a rotary evaporator (Hei-VAP Advantage ML/HB/G3, Heidolph, Schwabach, Germany). A volume of 40 ml absolute ethanol was then added to the concentrated solution to precipitate amylopectin. The amylopectins were lyophilized and their contents were determined by the previously published method [21]. In this study, the contents of kudzu and lotus rhizome amylopectins was (92.64 ± 0.08) g·kg^{-1} and (95.02 ± 0.05) g·kg^{-1}, respectively.

Preparation of ϕ,β-limit dextrins from amylopectins

According to the previously published method [22] with minor modifications, kudzu amylopectin or lotus rhizome amylopectin (1.0 g, dry basis) were dissolved in 50 ml of 90% dimethyl sulfoxide at room temperature for 60 min with constant stirring. A volume of 0.4 ml of rabbit muscle phosphorylase α (9 U·ml^{-1}) was mixed with 0.01 mol·l^{-1} sodium acetate buffer (pH 6.9; Huanling Chemi-

cal, Changzhou, China). The mixed solution was incubated at 37 °C for 12 h and then the enzyme reaction was stopped by boiling for 15 min. D-Glucose 1-phosphate produced was removed by using a tangential-flow filtration with an Omega 10 K membrane in a Minimate TFF capsule system (Pall Life Sciences, Ann Arbor, Michigan, USA). Phosphorolysis was carried out once more to gain ϕ-limit dextrins. Subsequently, the ϕ-limit dextrins were hydrolysed with 0.45 ml β-amylase (9 U·ml^{-1}) in 0.01 mol·l^{-1} sodium acetate buffer (pH 4.8) and incubated at 40 °C for 5 h to remove external chains. The hydrolysate solution was boiled for 15 min to inactivate the enzyme. A volume of 0.35 ml β-Amylase (9 U·ml^{-1}) was added to the hydrolysate solution and the solution was incubated at 40 °C for 3 h to ensure complete removal of the remaining external chains. The hydrolysis reaction was terminated by boiling for 15 min. Finally, the hydrolysate was dialysed with dialysis membranes MD55 (Solarbio, Beijing, China, molecular weight cut off 3500 Da) in deionized water to remove maltose and salt ions. The ϕ,β-limit dextrins obtained were lyophilized and stored at –18 °C.

Chain length distribution of amylopectins and ϕ,β-limit dextrins

Amylopectins or ϕ,β-limit dextrins (2.0 mg) were dissolved in 150 μl of 90% dimethyl sulfoxide at 100 °C with constant stirring for 30 min, respectively. The dispersion was diluted with 800 μl warm water and 100 μl of 0.1 mol·l^{-1} sodium acetate buffer (pH 5.5) containing 0.2 ml of 10% sodium azide to inhibit microbial growth. Then, 1 μl isoamylase and 1 μl pullulanase were added to the dispersion at room temperature. The debranching reaction was initiated at 25 °C with constant stirring for 12 h and then the reaction was terminated by heating at 100 °C for 20 min. The hydrolysates were diluted to a concentration of 1.0 mg·ml^{-1} with distilled water. An aliquot of 50 μl was filtered using a 0.45 μm organic acetylcellulose membrane filter (Solarbio) and then analysed using HPAEC-PAD on a Dionex ICS 3000 instrument (Thermo Fisher Scientific, Sunnyvale, California, USA). The analytical column was CarboPac PA-100 anion-exchange column (250 mm × 4 mm, Thermo Fisher Scientific), coupled to a CarboPac PA-100 guard column (50 mm × 4 mm, Thermo Fisher Scientific). The injection volume was 25 μl and the flow rate was 0.5 ml·min^{-1}. The hydrolysates were eluted at 0.5 ml·min^{-1} with a gradient of sodium acetate prepared by the mixture of eluent B (1 mol·l^{-1} sodium acetate) and eluent A (0.25 mol·l^{-1} sodium hydroxide) (composition given on v/v basis): 0 min to 15 min from 15 % to 34 %; 15 min to 26 min from 34 % to 40 %; 26 min to 52 min from 40 % to 49 %; 52 min to 54 min from 49 % to 100 %; 58 min to 60 min from 100 % to 15 %. Pulsed amperometric detection (PAD) signal was transformed into carbohydrate contents. Definition and method of calculation of all variables of chain length distributions are as follows:

External chain length (*ECL*)

$$ECL = CL_{\mathrm{ap}} - CL_{\mathrm{ld}} + 1.5 \quad (1)$$

where CL_{ap} is average chain length of amylopectin and CL_{ld} is average chain length of ϕ,β-limit dextrins.

Internal chain length (*ICL*)

$$ICL = CL_{\mathrm{ap}} - ECL - 1 \quad (2)$$

Total internal chain length (*TICL*)

$$TICL = BCL_{ld} - 1_{\ \mathrm{t}} \quad (3)$$

where BCL_{ld} is average chain length of B-chains calculated from ϕ,β-limit dextrin.

Number of chains (*NC*)

$$NC = \frac{DP_{\mathrm{ld}}}{CL_{\mathrm{ld}}} \quad (4)$$

where DP_{ld} is degree of polymerization of ϕ,β-limit dextrins.

Density of branch (*DB*)

$$DB = \frac{(NC - 1)}{DP_{\mathrm{ld}}} \times 100 \quad (5)$$

Number of chains per B-chain (NC_{B})

$$NC_{\mathrm{B}} = \frac{TICL}{(ICL + 1)} \quad (6)$$

ϕ,β-limit value (*LV*)

$$LV = 100 - 100 \times \frac{CL_{\mathrm{ld}}}{CL_{\mathrm{ap}}} \quad (7)$$

Hydrolysis of amylopectins using α-amylase and glucoamylase, individually and in combination

Digestibility

Lotus rhizome amylopectin or kudzu amylopectin (0.5 g, dry basis) were dissolved and uniformly stirred in 50 ml of 0.2 mol·l^{-1} acetate buffer (pH 6.0) containing 0.4 ml 10% sodium azide. α-Amylase (6.1 U·ml^{-1}) and glucoamylase (4.0 U·ml^{-1}), individually and in combination, were added to kudzu amylopectin or lotus rhizome amylopectin dispersions. The dispersions were incubated in a shaking water bath at 37 °C in the range of time from 0 h to 72 h. Aliquots (2 ml) of the hydrolysates were withdrawn at time intervals

(0, 5, 10, 15, 20, 25, 30, 40, 50, 60, 80, 100, 120, 240, 480, 1080, 1440, 2880, 3240 and 4320 min) and then immediately heated at 95 °C for 10 min to deactivate enzymes. Each aliquot was filtered using a 0.22 μm organic acetylcellulose membrane (Solarbio) to wipe off the non-reacted starch residue and the filtrate obtained was analysed for reducing sugars. The degree of hydrolysis is defined as the reducing sugars generated in supernatant, expressed as milligrams of maltose equivalents released per kilogram (dry weight) of amylopectin [23]. In this study, the contents of the free sugar in kudzu and lotus rhizome amylopectins were (1.38 ± 0.01) mg·kg^{-1} and (2.84 ± 0.02) mg·kg^{-1}, respectively. The contents of the free sugar were subtracted from total reducing sugars in the supernatant.

Logarithm of slope plot

A logarithm of slope plot has been effectively applied to predict digestion in human body and is determined by expressing the first derivative of the first-order equation (Eq. 8) in logarithmic form (Eq. 9) [24–26]:

$$C_t = C_\infty(1 - e^{-kt}) \quad (8)$$

$$\ln\left(\frac{dC}{dt}\right) = -kt + \ln(C_\infty k) \quad (9)$$

where t is digestion time (in minutes), C_t is product concentration (in grams per litre) at a given time (in minutes), C_∞ is product concentration (in grams per litre) at the end of the reaction, and k is digestion rate constant (in reciprocal minutes). A plot of $\ln(dC/dt)$ against t is linear with a slope ($-k$). The intercept on the y axis equals to $\ln(C_\infty k)$ and C_∞ is calculated from the value of k obtained from the slope of the plot. Based on the enzyme-kinetic principles, a logarithm of slope plot uses two variables (C_∞ and k) to precisely manifest the hydrolysed products released by amylolysis [27, 28]. A logarithm of slope plot can supply two or more distinct linear phases. The slope of each distinct phase can give the rate constant such as k_1, k_2…..etc., accordingly obtaining the end-point of starch amylolysis ($C_{1\infty}$, $C_{2\infty}$….etc.) to be calculated [26, 28].

Oligosaccharides released from amylopectins using amylases

The oligosaccharides released from kudzu and lotus rhizome amylopectins using α-amylase and glucoamylase (in percent, w/w), individually or in combination, were determined using a Waters 1500 HPLC system (Waters, Milford, Massachusetts, USA) equipped with a refractive index detector (RID, Waters 2414) and a Sugarpak column (300 mm × 6.5 mm, Waters). The mobile phase was ultrapure water at a flow rate of 0.5 ml·min^{-1}. The injection volume was 10 μl. The hydrolysates were dissolved in ultrapure water and then centrifuged for 20 min at 10000×g. The supernatant was filtered using a 0.22 μm organic acetylcellulose membrane filter (Solarbio), and then injected into the HPLC system. The quantities of oligosaccharides produced were calculated from a calibration curve constructed with a mixture of standards.

Statistical analysis

All analyses were done in triplicate. The results were expressed as mean ± standard deviation and were analysed using analysis of variance and Students t-test. Each hydrolysis treatment against time was analysed using Prism 7 (GraphPad Software, La Jolla, California, USA).

RESULTS AND DISCUSSION

Molecular structures of amylopectin and ϕ,β-limit dextrins

According to the division suggested by a previous report [29], the molar-based chain-length distribution of debranched amylopectins is grouped into four fractions: fraction A-chains (Fa) with a degree of polymerization (*DP*) of 6–12; fraction B1-chains (Fb1), or short B-chains (*DP* of 3–24); fraction B2-chains (Fb2) or long B-chains (*DP* of 25–36); and fraction B3-chains (Fb3) or longer B-chains (*DP* > 36). Fig. 1 depicts the molar-based chain-length profile of debranched amylopectins. Fig. 1A demonstrates that the first peak of molar-based bimodal chain-length profiles for kudzu amylopectin was the largest fraction at *DP* of 12. The second peak was at *DP* 47, which is in agreement with previous reports [11, 30]. The proportion of short B-chains (*DP* of 3–24) and long B-chains (*DP* of 25–36) quickly and slowly decreased, respectively, and a small increase in longer chain length (*DP* > 36) occured, which is in agreement with a previous report [30]. Similarly, Fig. 1B shows that the first peak of molar-based bimodal chain-length profiles for lotus rhizome amylopectin was the largest fraction at *DP* of 12, and the second peak was at *DP* of 43. An obvious decrease in the proportion of short B-chains with a little decrease in the proportion of long B-chains, and a small increase in longer chain length (*DP* > 36) occured. The quantitative results are depicted in Tab. 1. Compared to lotus rhizome amylopectin, kudzu amylopectin possessed a lower

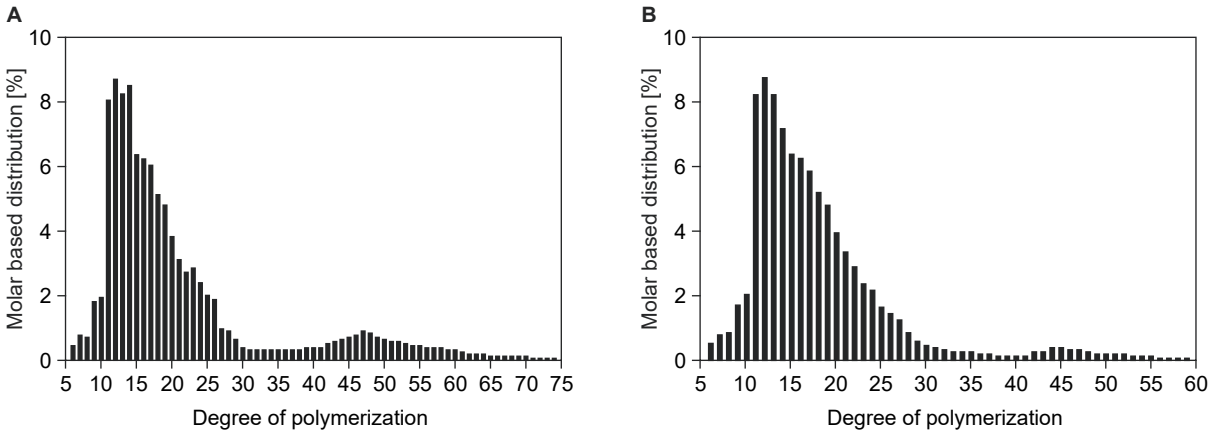

Fig. 1. Unit chain length distribution of debranched amylopectins.

A – kudzu amylopectin; B – lotus rhizome amylopectin.

molar-based ratio of fractions Fa (*DP* of 6–12) and Fb1 (*DP* of 13–24), and a higher molar-based ratio of fractions Fb2 (*DP* of 25–36) and Fb3 (*DP* > 36). More detailed information on linear chain lengths of amylopectin indicated that kudzu amylopectin had a higher average chain length (*CL*) expressed as multiplying degree of polymerization by the peak area corresponding to each *DP* (25.13), long chain length (*LCL*, 58.43), external chain lengths (*ECL*, 21.47), internal chain length (*ICL*, 2.66) and total internal chain length (*TICL*, 15.02) than lotus rhizome amylopectin (*CL* 19.12, *LCL* 52.26, *ECL* 15.70, *ICL* 2.42, *TICL* 13.54). On the other hand, kudzu amylopectin had lower short chain length (*SCL*, 12.57) than that of lotus rhizome amylopectin (*SCL* 15.82). These data indicate

Tab. 1. Chain length distribution.

Chain categories	Kudzu amylopectin	Lotus rhizome amylopectin
Debranched amylopectins		
A-chains (*DP* 6–12) [%]	19.6 ± 0.6	21.2 ± 0.2
Short B-chains (*DP* 13–24) [%]	42.3 ± 0.2	45.4 ± 0.4
Long B-chains (*DP* 25–36) [%]	14.6 ± 0.5	13.3 ± 0.5
Longer B-chains (*DP* >36) [%]	23.5 ± 0.5	20.1 ± 0.3
Average chain length	25.13 ± 0.32	19.12 ± 0.35
Average chain length of short chains (*DP* 6–36)	12.57 ± 0.37	15.82 ± 0.52
Average chain length of long chains (*DP* > 36)	58.43 ± 0.63	52.26 ± 0.42
External chain length	21.47 ± 0.51	15.70 ± 0.4
Internal chain length	2.66 ± 0.20	2.42 ± 0.62
Total internal chain length	15.02± 0.33	13.54 ± 0.54
Debranched ϕ,β-limit dextrins		
Degree of polymerization	18.46 ± 0.32	16.53 ± 0.24
Average chain length	5.16 ± 0.31	4.92 ± 0.70
Number of chains	3.58 ± 0.26	3.36 ± 0.23
Chain length of B-chains	16.02 ± 0.35	14.54 ± 0.42
Density of branch [%]	14.0 ± 0.5	14.3 ± 0.3
Number of chains per B-chain	4.10 ± 0.34	3.96 ± 0.16
ϕ,β-limit value [%]	79.5 ± 0.4	74.3 ± 0.2
Short B-chains (*DP* 3–22) [%]	64.9 ± 0.9	70.9 ± 0.6
Long B-chains (*DP* > 22) [%]	5.3 ± 0.3	3.4 ± 0.5
Ratio of short B-chains to long B-chains	12.25 ± 0.50	20.85 ± 0.34

that kudzu amylopectin possessed a higher long-to-short chain ratio than that of lotus rhizome amylopectin. The information about the internal structure of amylopectin can be obtained through the structure of B-chains of debranched ϕ,β-limit dextrins [31]. ϕ,β-Limit dextrins derived from amylopectin were analysed by HPAEC (Fig. 2). Fig. 2A regards ϕ,β-limit dextrins from kudzu amylopectin, more than one peak being shown at $DP > 13$. For ϕ,β-limit dextrins from lotus rhizome amylopectin, two or three peaks at $DP > 9$ are indicated in Fig. 2B. The linear dextrins (named group 1) consist of glucose, maltose and maltotriose, which derive from the interblock segments and are used for the estimation of interblock chain length (*IB-CL*). Group 1 elutes in front of the branched building blocks ($DP \leq 5$). Group 2 building blocks, which are most abundant (> 50 % by number) consist of only 2 chains with a *DP* of 5–9. Group 3 building blocks (with 3 chains, *DP* of 10–14) are the second most common group, and group 4 building blocks have *DP* of 15–19 [31]. It is obvious from Fig. 2C that, in comparison with ϕ,β-limit dextrins from kudzu amylopectin, lotus rhizome amylopectin possesses greater amounts at $DP < 10$, and that group 3 and group 4 in lotus rhizome amylopectin are lower than that in kudzu amylopectin, which indicates that the amount of long chains of ϕ,β-limit dextrins in lotus rhizome amylopectin was lower than that in kudzu amylopectin. The corresponding data of ϕ,β-limit dextrins of kudzu and lotus rhizome amylopectins are shown in Tab. 1. It is shown that average degree of polymerization (DP_{ld} 18.46), average chain length (CL_{ld} 5.16) and average number of chains (NC_{ld} 3.58) of kudzu amylopectin were greater than those of lotus rhizome amylopectin (DP_{ld} 16.53, CL_{ld} 4.92, NC_{ld} 3.36), which suggests that kudzu amylopectin has larger building blocks. The internal chains are composed of B-chains (substituted with other chains), whereas all A-chains (unsubstituted and completely external) appear as maltosyl stubs. B-chains are divided into short and long chains [29, 31]. The average chain length of B-chains (BCL_{ld} 16.02) of kudzu amylopectin was higher than that of in lotus rhizome amylopectin (BCL_{ld} 14.54), whereas density of branch of kudzu amylopectin (DB_{ld} 14.0 %) was lower than that of lotus rhizome amylopectin (DB_{ld} 14.3 %). Besides, the average number of chains per B-chain (NC_B 4.10) and ϕ,β-limit value (*LV* 79.5 %) of kudzu amylopectin were greater than those of lotus rhizome amylopectin (NC_B 3.96, *LV* 74.3 %). Kudzu amylopectin had a smaller molar ratio of short to long B-chains (12.25) than lotus rhizome amylopectin (20.85). It indicates that kudzu amylopectin possessed significantly more long chains than lotus rhizome amylopectin. It was reported that a higher number of short chains in a cluster increases the number of access points for amylase reactions. High degree of hydrolysis is positively correlated with a high proportion of short amylopectin branch chains [32]. Thus, it is supposed that kudzu amylopectin may be more susceptible to hydrolysis by amylases than kudzu amylopectin due to a higher proportion of short chains.

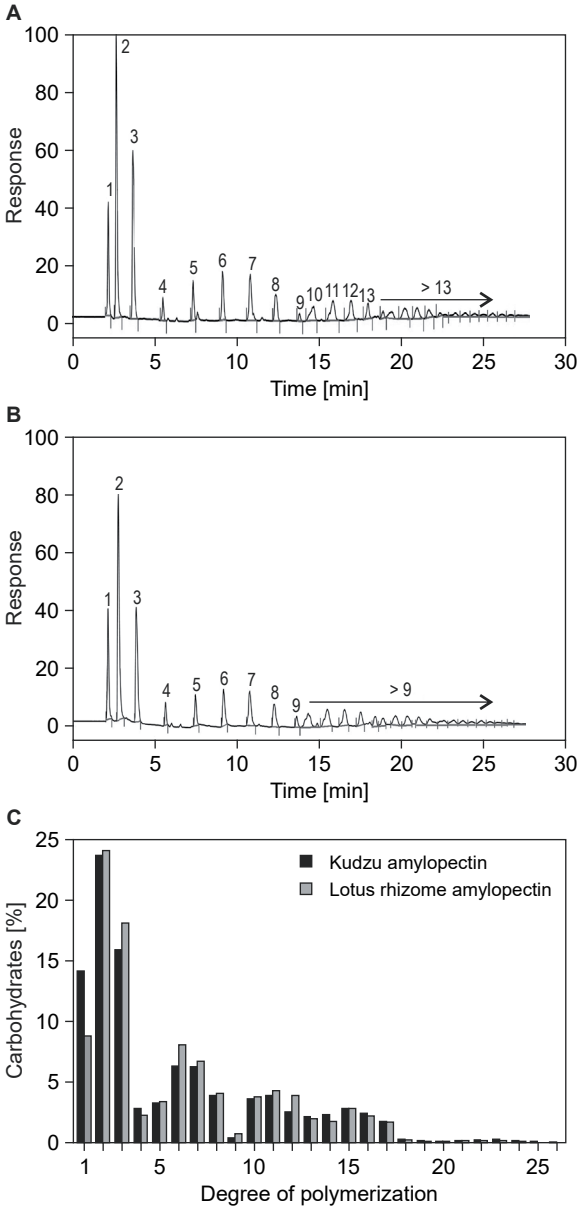

Fig. 2. High-performance anion-exchange chromatogram of debranched ϕ,β-limit dextrins.

A – kudzu amylopectin, B – lotus rhizome amylopectin, C – the quantitative bar.

Amylase hydrolysis of kudzu and lotus rhizome amylopectins

The hydrolysis plots of kudzu and lotus rhizome amylopectins using α-amylase and glucoamylase, individually and in combination, are shown in Fig. 3. At using α-amylase alone, kudzu and lotus rhizome amylopectins exhibited a rapid increase in hydrolysis with increasing incubation time at the early stage (0–120 min), and then smoothly increased to a plateau of 40.46 mg·kg^{-1} and 56.80 mg·kg^{-1}, respectively. At using both α-amylase and glucoamylase, kudzu and lotus rhizome amylopectins displayed a rapid increase in hydrolysis with increasing time at the early stage and then smoothly increased to a plateau of 48.28 mg·kg^{-1} and 63.77 mg·kg^{-1}, respectively. It indicated that kudzu and lotus rhizome amylopectin hydrolysis using α-amylase and glucoamylase was more effective than using α-amylase alone. This indicates synergism between α-amylase and glucoamylase in the hydrolysis of kudzu and lotus rhizome amylopectins, whereas the synergism for lotus rhizome amylopectin is more significant than the synergism for kudzu amylopectin. Fig. 3 demonstrates that when using α-amylase and glucoamylase individually or in combination, kudzu amylopectin was hydrolysed slower than lotus rhizome amylopectin at each time point, indicating that kudzu amylopectin was less susceptible to α-amylase and glucoamylase. This could be partially due to the different chain length distribution in kudzu and lotus rhizome amylopectins as discussed above. Compared to kudzu amylopectin, lotus rhizome amylopectin possesses higher numbers of short chains causing more non-reducing ends exposed to the action of amylase, which results in an increased accessibility of amylases towards the glycosidic bonds [32]. Also, in terms of amylopectin chain length, kudzu amylopectin has longer chain length, long chain length, external chain length, internal chain length and total internal chain length than lotus rhizome amylopectin. Longer chains would make long helices and strengthen hydrogen bonds between chains, which could retard enzymatic hydrolysis, whereas a high proportion of shorter chains forming short or weak double helices, inversely affects digestibility [11]. It confirms that the property of slow digestibility may arise from the rate-limiting step in enzyme hydrolysis of amylopectins with higher proportions of long chains.

Logarithm of slope analysis

A logarithm of slope plot is used to determine single-phase or two-phase amylolysis through a digestibility curve obtained experimentally. Fig. 4 shows that a logarithm of slope plots of kudzu and lotus rhizome amylopectins digestibility data were linear ($R^2 > 0.9$), characterized by single and two rate constants. Kudzu amylopectin displayed a single-phase plot, whereas lotus rhizome amylopectin indicated a two-phase process. A logarithm of slope plot is composed of two linear phases, each identified by a rate constant (k and C_∞). Fig. 4A and 4B present a single rate constant obtained by using a single-phase process for kudzu amylopectin amylolysis. Fig. 4C and 4D imply a discontinuity, indicating that lotus rhizome amylopectin was digested in a two-phase process, as two sets of k and C_∞ values were required to describe each amylolysis phase. The point at which the slower phase became the dominant reaction is expressed by the intersection between the two linear phases of a logarithm of slope plot [27]. Fig. 4C reveal that, for lotus rhizome amylopectin hydrolysed by α-amylase alone, the faster phase was of a short duration of approximately 25 min, which was then succeeded by the slower phase. Com-

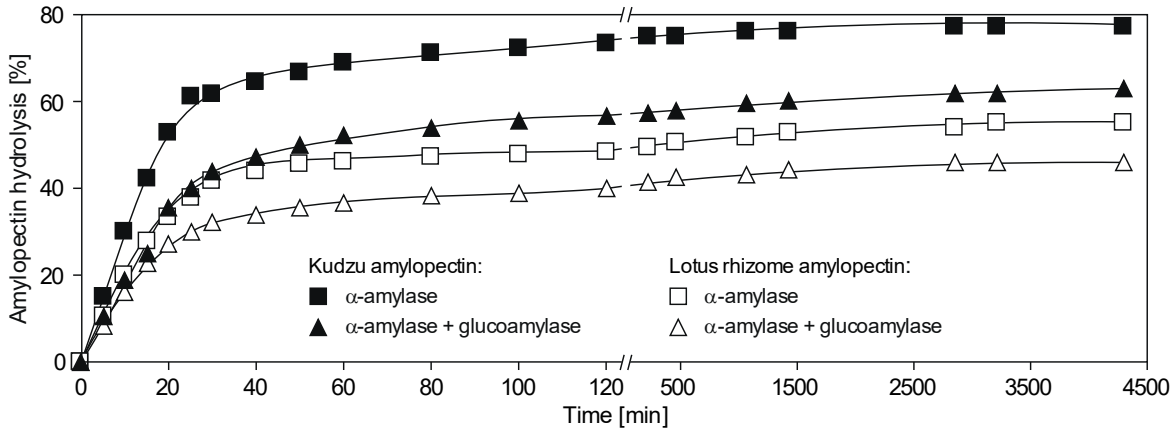

Fig. 3. Hydrolysis of amylopectins using α-amylase and glucoamylase.

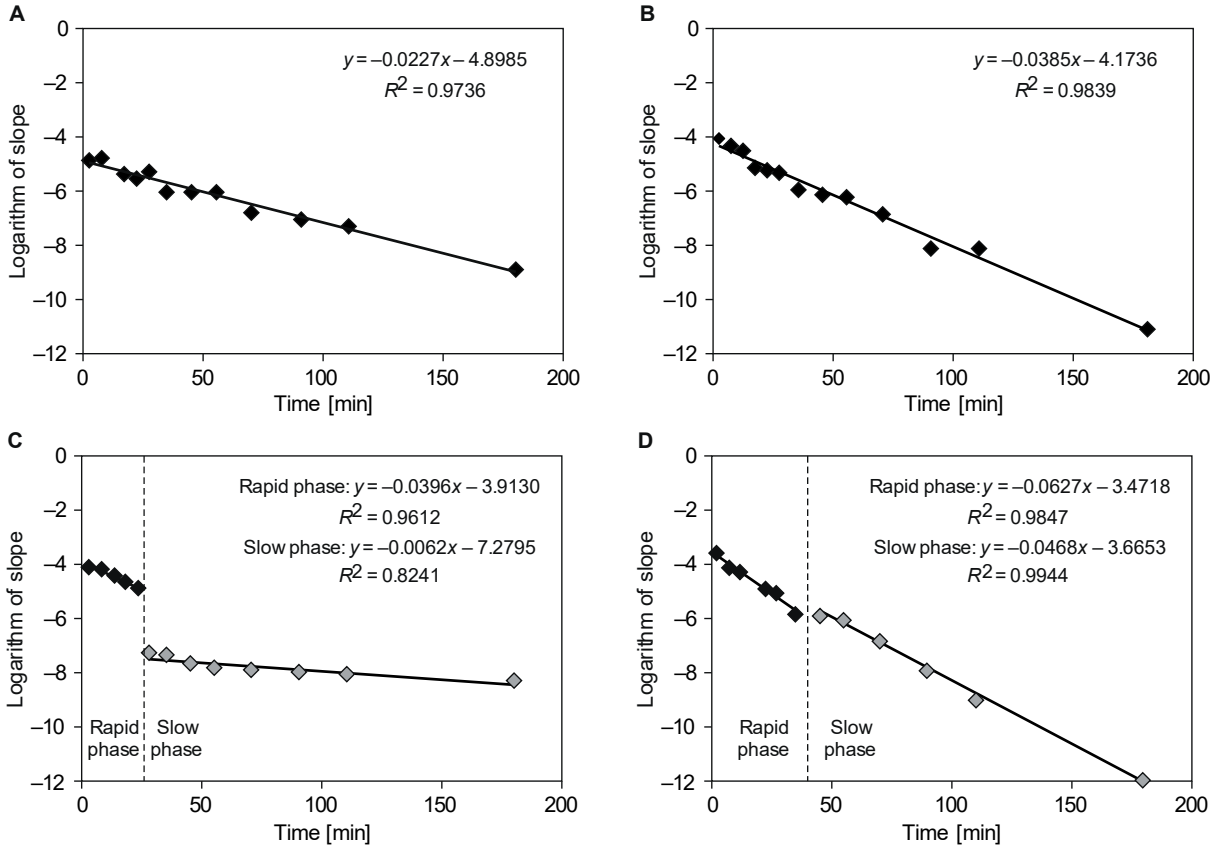

Fig. 4. Logarithm of slope plots obtained for amylopectins.

A – Kudzu amylopectin amylosis using α-amylase, B – Kudzu amylopectin amylosis using α-amylase and glucoamylase, C – lotus rhizome amylopectin amylosis using α-amylase, D – lotus rhizome amylopectin amylosis using α-amylase and glucoamylase.

paratively, Fig. 4D indicate that, in case of lotus rhizome amylopectin hydrolysed by α-amylase and glucoamylase, the more rapid phase was of relatively long (lasting for 35 min) and then was followed by the slower phase. The faster phase (k_1 and $C_{1\infty}$) denoted accessible chains and the slower phase (k_2 and $C_{2\infty}$) represented the less accessible α-glucan chains [26]. The rapid-phase (k_1 and $C_{1\infty}$) and slow-phase (k_2 and $C_{2\infty}$) values were calculated from *y*-intercept and slope in the logarithm of slope plots. Generally, the first reaction rate (k_1) is higher than the second reaction rate (k_2). Values of k and C_∞ calculated are listed in Tab. 2. For using α-amylase and glucoamylase individually or in combination, k_1 values for the rapidly hydrolysable kudzu and lotus rhizome amylopectins were higher than k_2 values for the slowly hydrolysable kudzu and lotus rhizome amylopectins. Using α-amylase and glucoamylase individually or in combination, k values of kudzu amylopectin

Tab. 2. Values of variables estimated from a logarithm of slope analysis.

Amylopectin	Enzymes	Rapid phase		Single or slow phase	
		k_1 [min^{-1}]	$C_{1\infty}$ [g·l^{-1}]	k_2 [min^{-1}]	$C_{2\infty}$ [g·l^{-1}]
Kudzu	α-amylase	–	–	0.023*	0.329*
	α-amylase and glucoamylase	–	–	0.039*	0.400*
Lotus rhizome	α-amylase	0.040	0.505	0.006	0.111
	α-amylase and glucoamylase	0.063	0.495	0.047	0.547

Values are determined from a logarithm of slope plots with one or two-phases.
k – digestion rate constant. C_∞ – product concentration at the end of the reaction, * – amylolysis occured by a single-phase process, no rapid phase was observed.

were lower than those of lotus rhizome amylopectin. The lower k value of kudzu amylopectin may be explained by the slow rate of diffusion of amylase through its more stable long-chains structure to reach glucan chains. The $C_{1\infty}$ and $C_{2\infty}$ values indicate the contribution of each amylolysis phase to the enzyme hydrolysis of amylopectins [27]. For lotus rhizome amylopectin using α-amylase alone, the rapid reaction ($C_{1\infty} > C_{2\infty}$) was the greater contributor to total amylopectin amylolysis, whereas for lotus rhizome amylopectin hydrolysis by α-amylase and glucoamylase, the slower reactions ($C_{1\infty} < C_{2\infty}$) were the larger contributors to total amylopectin amylolysis.

Oligosaccharides released from kudzu and lotus rhizome amylopectins using amylases

The oligosaccharides of kudzu and lotus rhizome amylopectins released using α-amylase and glucoamylase, individually or in combination, are depicted in Fig. 5. Maltopentaose could not be detected during the whole hydrolysis period for kudzu and lotus rhizome amylopectins. Fig. 5A shows that, for kudzu amylopectin hydrolysed with α-amylase alone, a small amount of glucose release during the whole hydrolysis time. Glucose enhanced as the incubation time increased at the slowest rate. Maltose obviously increased with increasing time during the whole incubation time. Maltotriose and maltotetraose increased with increasing the incubation time (≤ 8 h) and then decreased. Maltohexaose gradually decreased with increasing the incubation time, whereas maltoheptaose significantly decreased with increasing the incubation time. Together with glucoamylase, the hydrolysis behaviour of glucose and six maltooligosaccharides from kudzu amylopectin is shown in Fig. 5B. It demonstrates that, in contrast with kudzu amylopectin hydrolysis using α-amylase alone, glucose more significantly increased with increasing the incubation time at the highest rate. Maltose increased with increasing time during the whole incubation. Maltotriose increased with increasing incubation time (≤ 18 h) and then decreased. Maltotetraose and maltohexaose increased at the early stage (≤ 60 min) and then decreased. Maltoheptaose obviously decreased with increasing incubation time. Fig. 5C shows that, similarly to kudzu amylopectin hydrolysis using α-amylase alone, a small amount of glucose was produced from lotus rhizome amylopectin. Glucose and maltose increased with increasing incubation time. Maltotriose increased with increasing incubation time (≤ 18 h) and then decreased. Maltotetraose enhanced with increasing incubation time (≤ 120 min) and then obviously decreased. Maltohexaose increased with increasing time at initial stage (≤ 20 min) and then decreased to zero. Maltoheptaose significantly decreased with increasing incubation time. Fig. 5D depicts that, for lotus rhizome amylopectin hydrolysis using α-amylase and glucoamylase, glucose most significantly increased with increasing incubation time at the highest rate. Maltose gradually increased with increasing incubation time. Maltotriose increased with increasing time until 8 h, and then rapidly decreased. Maltotetraose and maltohexaose decreased to zero with increasing incubation time. Maltoheptaose obviously decreased with increasing incubation time. In short, glucose releases slightly when kudzu and lotus rhizome amylopectins are hydrolsed by α-amylase alone. Maltose, maltotriose and maltotetraose were produced from larger maltodextrins at the initial or middle stage, and they were further hydrolysed to glucose by glucoamylase at the late stage. As expected, very little glucose was released from kudzu and lotus rhizome amylopectins with α-amylase alone, the primary products being maltose, maltotriose and maltotetraose. Using α-amylase and glucoamylase, much more glucose was produced from kudzu and lotus rhizome amylopectins indicating that glucose release depended on glucoamylase action. Synergism occured between α-amylase and glucoamylase in glucose released from kudzu and lotus rhizome amylopectins, and it improved remarkably with increasing hydrolysis time. It indicates that glucoamylase converts efficiently inhibitory oligosaccharides produced by α-amylase into glucose. This is in accordance with data from previous studies regarding the synergism in the action of α-amylase and glucoamylase when they hydrolyse starches. The synergism can be explained by the fact that glucoamylase can directly attack starch granules and break down the oligosaccharides produced by α-amylase [33, 34]. Compared to kudzu and lotus rhizome amylopectins hydrolysed by α-amylase and glucoamylase, individually or in combination, the amount of glucose released from lotus rhizome amylopectin was significantly higher due to a high proportion of shorter chains. Relatively high-molecular-weight oligosaccharides such as maltohexaose and maltoheptaose were reduced with increasing incubation time. It further verified that maltohexaose and maltoheptaose are ideal hydrolytic substrates that accordingly produce maltose + maltotetraose and maltose + maltopentaose. Subsequently, maltotetraose and maltopentaose are degraded into glucose + maltotriose and maltose + maltotriose, respectively. Eventually, maltotriose and maltotetraose are hydrolysed into glucose and maltose. This is

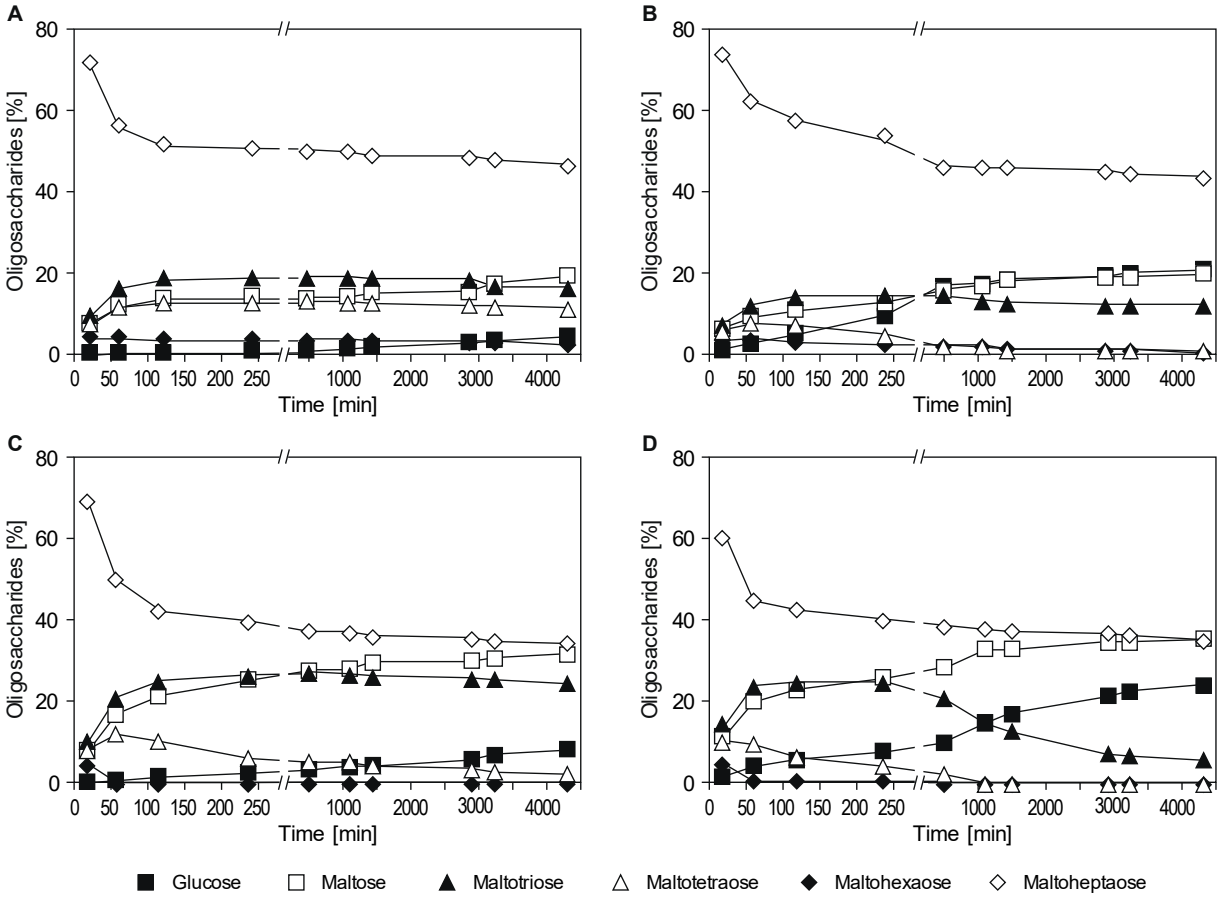

Fig. 5. Time course of oligosaccharides release from amylopectins.

A – Kudzu amylopectin amylosis using α-amylase, B – Kudzu amylopectin amylosis using α-amylase and glucoamylase, C – lotus rhizome amylopectin amylosis using α-amylase, D – lotus rhizome amylopectin amylosis using α-amylase and glucoamylase.

because α-amylase from *Bacillus amyloliquefaciens* possesses nine subsite binding sites with the catalytic groups located between subsite-3 and subsite-4, producing three subsites to the right and six subsites to the left of the catalytic site [7, 35]. Thus, it is obvious that glucose is not the primary product, whereas glucose is released as a secondary product in the hydrolysis of maltohexaose and maltoheptaose. The above results coincide with previous reports [36–38].

CONCLUSIONS

The study was conducted to understand the relationship between molecular structure and degree of amylolysis in amylopectins from kudzu and lotus rhizome starches. The difference in degree of hydrolysis during the initial stages of amylolysis using α-amylase and glucoamylase, individually and in combination, reflected variations in amylopectin chain length distribution. High degree of hydrolysis of lotus rhizome amylopectin was correlated with a high proportion of short amylopectin branch chains. The low hydrolysis rate of kudzu amylopectin may be attributed to the presence of higher numbers of long chains, the lower rate of amylolysis being ideal for the development of low-glycemic foods. Significant correlations between the chain length distribution and enzymatic hydrolysis of amylopectin were observed. These indicate that amylopectin structural parameters are important factors determining digestibility of kudzu and lotus rhizome amylopectins. Kudzu amylopectin displayed single-phase mechanisms, whereas lotus rhizome amylopectin was digested in two phases, as demonstrated by logarithm of slope plots. The *k* value of kudzu amylopectin was lower than that of lotus rhizome amylopectin. When α-amylase was used alone, only a small amount of glucose was produced from kudzu and lotus rhizome amylopectins. On the other hand,

when used together with glucoamylase, the release of glucose significantly enhanced, suggesting that glucose release is dependent on the action of glucoamylase, and that there is synergism between α-amylase and glucoamylase.

Acknowledgements

This research was supported by National Natural Science Foundation of China (Grant No. 31771933), International Cooperation Foundation of Qilu University of Technology (Shandong Academy of Sciences, Grant No. 450401) and Special Funds for Taishan Scholars.

REFERENCES

1. Geng, Z. – Zongdao, C. – Yimin, W.: Physicochemical properties of lotus (*Nelumbo nucifera* Gaertn.) and kudzu (*Pueraria hirsute* Matsum.) starches. International Journal of Food Science and Technology, *42*, 2007, pp. 1449–1455. DOI: 10.1111/j.1365-2621.2006.01363.x.
2. Guo, L. – Hu, J. – Zhou, X. – Li, X. L. – Du, X. F.: In vitro digestibility of kudzu starch by using α-amylase and glucoamylase. Starch/Stärke, *68*, 2016, pp. 140–150. DOI: 10.1002/star.201500213.
3. Chen, G. – Zhang, J. – Ye, J.: Determination of puerarin, daidzein and rutin in *Pueraria lobata* (Wild.) Ohwi by capillary electrophoresis with electrochemical detection. Journal of Chromatography A, *923*, 2001, pp. 255–262. DOI: 10.1016/S0021-9673(01)00996-7.
4. Suzuki, A. – Hizukuri, S. – Takeda, Y.: Physicochemical studies of kudzu starch. Cereal Chemistry, *58*, 1981, pp. 286–290. ISSN: 0009-0352.
5. Zhu, F.: Structures, properties, and applications of lotus starches. Food Hydrocolloids, *63*, 2017, pp. 332–348. DOI: 10.1016/j.foodhyd.2016.08.034.
6. Singh, J. – Dartois, A. – Kaur, L.: Starch digestibility in food matrix: a review. Trends in Food Science and Technology, *21*, 2010, pp. 168–180. DOI: 10.1016/j.tifs.2009.12.001.
7. Whistler, R. L. – BeMiller, J. M. – Paschall, E. F. (Eds.): Starch: Chemistry and technology. 2nd edition. San Diego : Academic Press, 1984. ISBN: 0-12-746270-8.
8. Hung, P. V. – Morita, N.: Chemical compositions, fine structure and physicochemical properties of kudzu (*Pueraria lobata*) starches from different regions. Food Chemistry, *105*, 2007, pp. 749–755. DOI: 10.1016/j.foodchem.2007.01.023.
9. Zhang, B. – Wu, C. S. – Li, H. Y. – Hu, X. T. – Jin, Z. Y. – Tian, Y. Q. – Xu, X. M.: Long-term annealing of C-type kudzu starch: Effect on crystalline type and other physicochemical properties. Starch/Stärke, *67*, 2015, pp. 577–584. DOI: 10.1002/star.201500003.
10. Lin, L. S. – Huang, J. – Zhao, L. X. – Wang, J. – Wang, Z. F. – Wei, C. X.: Effect of granule size on the properties of lotus rhizome C-type starch. Carbohydrate Polymers, *134*, 2015, pp. 448–457. DOI: 10.1016/j.carbpol.2015.08.026.
11. Srichuwong, S. – Sunarti, T. C. – Mishima, T. – Isono, N. – Hisamatsu, M.: Starches from different botanical sources I: Contribution of amylopectin fine structure to thermal properties and enzyme digestibility. Carbohydrate Polymers, *60*, 2005, pp. 529–538. DOI: 10.1016/j.carbpol.2005.03.004.
12. Bertoft, E.: On the building block and backbone concepts of amylopectin structure. Cereal Chemistry, *90*, 2013, pp. 294–311. DOI: 10.1094/CCHEM-01-13-0004-FI.
13. Kong, X. L. – Bertoft, E. – Bao, J. S. – Corke, H.: Molecular structure of amylopectin from amaranth starch and its effect on physicochemical properties. International Journal of Biological Macromolecules, *43*, 2008, pp. 377–382. DOI: 10.1016/j.ijbiomac.2008.07.018.
14. O'Sullivan, A. C. – Pérez, S.: The relationship between internal chain length of amylopectin and crystallinity in starch. Biopolymers, *50*, 1999, pp. 381–390. DOI: 10.1002/(SICI)1097-0282(19991005)50:4<381::AID-BIP4>3.0.CO;2-W.
15. Pérez, S. – Bertoft, E.: The molecular structures of starch components and their contribution to the architecture of starch granules: A comprehensive review. Starch/Stärke, *62*, 2010, pp. 389–420. DOI: 10.1002/star.201000013.
16. Vamadevan, V. – Bertoft, E.: Structure-function relationships of starch components. Starch/Stärke, *67*, 2015, pp. 55–68. DOI: 10.1002/star.201400188.
17. Zhu, F. – Corke, H. – Bertoft, E.: Amylopectin internal molecular structure in relation to physical properties of sweet potato starch. Carbohydrate Polymers, *84*, 2011, pp. 907–918. DOI: 10.1016/j.carbpol.2010.12.039.
18. Zhang, B. – Dhital, S. – Gidley, M. J.: Synergistic and Antagonistic Effects of α-amylase and amyloglucosidase on starch digestion. Biomacromolecules. *14*, 2013, pp. 1945–1954. DOI: 10.1021/bm400332a.
19. Somogyi, M. J.: Notes on sugar determination. Journal of Biological Chemistry, *195*, 1952, pp. 19–25. ISSN: 0021-9258.
20. Bijttebier, A. – Goesaert, H. – Delcour, J. A.: Amylase action pattern on starch polymers. Biologia, *63*, 2008, pp. 989–999. DOI: 10.2478/s11756-008-0169-x.
21. Wang, J. P. – Yu, B. – Xu, X. M. – Yang, N. – Jin, Z. Y. – Kim, J. M.: Orthogonal-function spectrophotometry for the measurement of amylose and amylopectin contents. Food Chemistry, *127*, 2011, pp. 102–108. DOI: 10.1016/j.foodchem.2010.12.094.
22. Laohaphatanaleart, K. – Piyachomkwan, K. – Sriroth, K. – Santisopasri, V. – Bertoft, E.: A study of the internal structure in cassava and rice amylopectin. Starch/Stäke, *61*, 2009, pp. 557–569. DOI: 10.1002/star.200900154.
23. Guo, L. – Zhang, J. J. – Hu, J. – Li, X. L. – Du, X. F.: Susceptibility of glutinous rice starch to digestive enzymes. Carbohydrate Polymers, *128*, 2015, pp. 154–162. DOI: 10.1016/j.carbpol.2015.04.008.
24. Dona, A. C. – Pages, G. – Gilbert, R. G. – Kuchel, P. W.: Digestion of starch: In vivo and in vitro

kinetic models used to characterise oligosaccharide or glucose release. Carbohydrate Polymers, *80*, 2010, pp. 599–617. DOI: 10.1016/j.carbpol.2010.01.002.
25. Goňi, I. – Garcia-Alonso, A. – Saura-Calixto, F.: A starch hydrolysis procedure to estimate glycemic index. Nutrition Research, *17*, 1997, pp. 427–437. DOI: 10.1016/S0271-5317(97)00010-9.
26. Butterworth, P. J. – Warren, F. J. – Grassby, T. – Patel, H. – Ellis, P. R.: Analysis of starch amylolysis using plots for first-order kinetics. Carbohydrate Polymers, *87*, 2012, pp. 2189–2197. DOI: 10.1016/j.carbpol.2011.10.048.
27. Edwards, C. H. – Warren, F. J. – Milligan, P. J. – Butterworth, P. J. – Ellis, P. R.: A novel method for classifying starch digestion by modelling the amylolysis of plant foods using first-order enzyme kinetic principles. Food and Function, *5*, 2014, pp. 2751–2758. DOI: 10.1039/c4fo00115j.
28. Patel, H. – Day, R. – Butterworth, P. J. – Ellis, P. R.: A mechanistic approach to studies of the possible digestion of retrograded starch by α-amylase revealed using a log of slope (LOS) plot. Carbohydrate Polymers, *113*, 2014, pp. 182–188. DOI: 10.1016/j.carbpol.2014.06.089.
29. Hanashiro, I. – Tagawa, M. – Shibahara, S. – Iwata, K. – Takeda, Y.: Examination of molar-based distribution of A, B and C chains of amylopectin by fluorescent labeling with 2-aminopyridine. Carbohydrate Research, *337*, 2002, pp. 1211–1215. DOI: 10.1016/S0008-6215(02)00110-6.
30. Yoo, S. H. – Perera, C. – Shen, J. – Ye, L. – Suh, D. S. – Jane, J. L.: Molecular structure of selected tuber and root starches and effect of amylopectin structure on their physical properties. Journal of Agricultural and Food Chemistry, *57*, 2009, pp. 1556–1564. DOI: 10.1021/jf802960f.
31. Bertoft, E. – Koch, K. – Åman, P.: Building block organisation of clusters in amylopectin from different structural types. International Journal of Biological Macromolecules, *50*, 2012, pp. 1212–1223. DOI: 10.1016/j.ijbiomac.2012.03.004.
32. Naguleswaran, S. – Vasanthan, T. – Hoover, R. – Bressler, D.: Amylolysis of amylopectin and amylose isolated from wheat, triticale, corn and barley starches. Food Hydrocolloids, *35*, 2014, pp. 686–693. DOI: 10.1016/j.foodhyd.2013.08.018.
33. Brewer, L. R. – Cai, L. – Shi, Y.-C.: Mechanism and enzymatic contribution to in vitro test method of digestion for maize starches differing in amylose content. Journal of Agricultural and Food Chemistry, *60*, 2012, pp. 4379–4387. DOI: 10.1021/jf300393m.
34. Kimura, A. – Robyt, J. F.: Reaction of enzymes with starch granules: Kinetics and products of the reaction with glucoamylase. Carbohydrate Research, *277*, 1995, pp. 87–107. DOI: 10.1016/0008-6215(95)00196-Z.
35. Yook, C. – Robyt, J. F.: Reactions of alpha amylases with starch granules in aqueous suspension giving products in solution and in a minimum amount of water giving products inside the granule. Carbohydrate Research, *337*, 2002, pp. 1113–1117. DOI: 10.1016/S0008-6215(02)00107-6.
36. Bijttebier, A. – Goesaert, H. – Delcour, J. A.: Hydrolysis of amylopectin by amylolytic enzymes: structural analysis of the residual amylopectin population. Carbohydrate Research, *345*, 2010, pp. 235–242. DOI: 10.1016/j.carres.2009.11.010.
37. Goesaert, H. – Bijttebier, A. – Delcour, J. A.: Hydrolysis of amylopectin by amylolytic enzymes: level of inner chain attack as an important analytical differentiation criterion. Carbohydrate Research, *345*, 2010, pp. 397–401. DOI: 10.1016/j.carres.2009.11.011.
38. Robyt, J. F. – French, D.: Action pattern and specificity of an amylase from *Bacillus subtilis*. Archives of Biochemistry and Biophysics, *100*, 1963, pp. 451–467. DOI: 10.1016/0003-9861(63)90112-7.

Received 18 January 2018; accepted 18 July 2018; published online 23 October 2018.